

# Characterization of Novel Phosphodiesterases in the Bovine Ovarian Follicle<sup>1</sup>

Maxime Sasseville,<sup>3,4</sup> Firas K. Albuz,<sup>4</sup> Nancy Côté,<sup>3</sup> Christine Guillemette,<sup>3</sup> Robert B. Gilchrist,<sup>4</sup> and François J. Richard<sup>2,3</sup>

Centre de Recherche en Biologie de la Reproduction,<sup>3</sup> Département des Sciences Animales, Université Laval, Sainte-Foy, Québec, Canada  
Robinson Institute,<sup>4</sup> School of Paediatrics and Reproductive Health, Medical School, University of Adelaide, Adelaide, South Australia, Australia

## ABSTRACT

The phosphodiesterase (PDE) family is a group of enzymes that catalyzes the transformation of cyclic nucleotides into 5' nucleotides. Based on rodents, the current mammalian model of PDE distribution in the ovarian follicle predicts *Pde3a* in the oocyte and *Pde4d* in the somatic cells. Using bovine as an experimental model, the present results showed that PDE3 was the predominant PDE activity in oocytes. However, cumulus cell cAMP-PDE activity was predominantly resistant to inhibition by 3-isobutyl-methylxanthine, indicating PDE8 activity (60% of total PDE activity) and a minor role for PDE4 (<5%). A total of 20% of total oocyte PDE activity was also attributed to PDE8. The PDE activity measurements in mural granulosa cells from 2 to 6 mm in diameter suggest the presence of PDE4 and PDE8. In granulosa cells from follicles >10 mm, total PDE and PDE8 activities along with PDE8A protein level were increased compared with smaller follicles. The RT-PCR experiments showed that cumulus cells expressed *PDE8A*, *PDE8B*, and *PDE10A*. Western blot experiments showed *PDE8A*, *PDE8B*, and *PDE4D* proteins in mural granulosa cells and cumulus-oocyte complexes. PDE8 inhibition using dipyrindamole in a dose-dependent manner increased cAMP levels in the cumulus-oocyte complexes and delayed oocyte nuclear maturation. These results are the first to demonstrate the functional presence of PDE8 in the mammalian ovarian follicle. This challenges the recently described cell-specific expression of cAMP-PDEs in the ovarian follicle and the notion that PDE4 is the predominant granulosa/cumulus cell PDE. These findings have implications for our understanding of hormonal regulation of folliculogenesis and the potential application of PDE inhibitors as novel contraceptives.

*cumulus cells, cyclic adenosine monophosphate, follicle, gamete biology, oocyte, phosphodiesterases, signal transduction*

<sup>1</sup>Supported by a Natural Science and Engineering Research Council of Canada (NSERC) postdoctoral fellowship to M.S.; an Australian Postgraduate Award Industry from the Australian Research Council to F.K.A.; the National Health and Medical Research Council of Australia's RD Wright Fellowship and a Program Grant to R.B.G.; and the NSERC and the Canadian Institutes for Health Research in the Program for Oocyte Health to F.J.R.

<sup>2</sup>Correspondence: François J. Richard, Centre de Recherche en Biologie de la Reproduction, Département des Sciences Animales, Université Laval, Sainte-Foy, QC, Canada G1V 0A6. FAX: 418 656 3766; e-mail: francois.richard@fsaa.ulaval.ca

Received: 26 October 2008.  
First decision: 15 November 2008.  
Accepted: 25 March 2009.

© 2009 by the Society for the Study of Reproduction, Inc.  
eISSN: 1259-7268 <http://www.biolreprod.org>  
ISSN: 0006-3363

## INTRODUCTION

Cyclic AMP is synthesized by the members of the adenylyl cyclase (*ADCY*) gene family and degraded to its inactive analogue 5'-AMP by phosphodiesterases (PDEs). Ten *ADCY* genes have been found in the human genome: nine membrane bound and one soluble. The 23 PDE genes are grouped as 11 families according to various properties, such as homology, substrate specificity, and activity regulation [1]. Tsafiriri et al. [2] have reported that the cellular localization of *Pde3a* is restricted to the oocyte, whereas *Pde4d* is detected in the granulosa/cumulus cell compartment in the rat ovary [2]. They have further demonstrated that the specific inhibition of the PDE3 family members could prevent spontaneous in vitro oocyte meiotic resumption to the same extent as a nonspecific PDE inhibitor, whereas specific inhibition of PDE4 did not [2]. Genetic disruption of *Pde3a* and *Pde4d* in mice have led to female infertility and impaired fertility, respectively, and have further shown the paramount importance of these two PDEs in ovarian physiology [3, 4]. These studies in rodents have allowed the establishment of a model of cell-specific expression of PDEs in the ovarian follicle, in which *Pde3a* is the major oocyte PDE and *Pde4d* the major granulosa cell PDE [5].

Mammalian oocytes initiate meiosis during fetal life but remain arrested at the diplotene stage of the first meiotic prophase until triggered to resume by the ovulatory luteinizing hormone pulse. We know from previous studies that high levels of 3'/5'-cAMP maintain oocytes in meiotic arrest by activating cAMP-dependant protein kinase, which prevents activation of maturation-promoting factor (MPF), a heterodimer of both cyclin B (*CCNB*) and cell division cycle 2 (*CDC2*, previously known as *CDK1*) [6]. Bovine oocytes, like all mammalian oocytes, resume meiosis spontaneously after retrieval from the ovarian follicular environment [7, 8]. This premature nuclear maturation compromises oocyte developmental capacity compared with in vivo counterparts [9–11]. Attempts to delay bovine oocyte nuclear maturation by modulating specific PDEs delay the rupture of gap-junctional communication between the oocyte and surrounding cumulus cells and improve the rate and quality of subsequent blastocyst development [12, 13].

In mouse, rat, and pig, both broad-spectrum PDE inhibitors and PDE3-specific inhibitors can reversibly hold oocytes in meiotic arrest in vitro [2, 14, 15]. In contrast, these inhibitors are only partially effective at preventing bovine oocyte meiotic resumption [8, 16–18]. Human oocytes recovered from unstimulated ovaries are only partially maintained in meiotic arrest by the PDE3 inhibitor cilostamide, either alone or in combination with the adenylyl cyclase activator forskolin, which suggests that mechanisms modulating cAMP in human oocytes may be more like those in bovine oocytes than those in

TABLE 1. Specificity of PDE inhibitors.

Inhibitor	cAMP-PDE families inhibited by	IC <sub>50</sub> [reference]	cAMP-PDE families NOT inhibited by	IC <sub>50</sub> [reference]
IBMX	PDE1	2–50 μM [24]	PDE8	>200 μM [24]
	PDE2			
	PDE3			
	PDE4			
	PDE7			
	PDE10			
Cilostamide	PDE11	20 nM [27]	PDE1	
	PDE3		PDE2	
			PDE4	
Rolipram	PDE4	1 μM [28]	PDE7	
			PDE8	
			PDE10	
			PDE11	
			PDE1	
			PDE2	
			PDE3	
			PDE7	
			PDE8	
			PDE10	
			PDE11	
Dipyridamole	PDE7	9–42 μM [30, 31]	PDE1	
	PDE8	4.5–9.0 μM [24, 29]	PDE2	
	PDE10	1.1 μM [32]	PDE3	
	PDE11	0.37–1.8 μM [30, 33]	PDE4	

mouse [19]. The reason for this species-specific difference is unknown. Moreover, the mechanism by which bovine and human oocytes are only transiently affected by PDE inhibitors remains to be determined. However, it is worth noting that translation inhibitors maintain nearly 100% of oocytes arrested for 24 h, suggesting that this mechanism is upstream of *CCNB* translation and MPF activation [20, 21].

The current PDE distribution model in the ovarian follicle is based mainly on observations in rodents. This study was designed to characterize the PDE distribution in bovine ovarian cell types to better understand the underlying cellular management of gonadotropin endocrine cues. Our results provide evidence of a new PDE expressed in the bovine ovarian follicle that might pave the way for novel contraceptives or gonadotropin sensitizers.

## MATERIALS AND METHODS

### Chemicals

Unless otherwise noted, all chemicals were bought from Sigma Chemical Co. (St. Louis, MO). All pharmacological inhibitors were stored in aliquots at –20°C until use.

### Tissue Recovery and Culture

Bovine ovaries were recovered from a local slaughterhouse and kept in 0.9% (w/v) NaCl solution with antibiotic and antimycotic agents at 37°C. Cumulus-oocyte complexes (COCs) and mural granulosa cells were recovered from 3- to 6-mm antral follicles (unless otherwise noted) using an 18-gauge needle attached to a 10-ml syringe. The COCs were kept in follicular fluid and selected for compact cumulus cells and a homogeneous oocyte cytoplasm. Mural granulosa cells were recovered from the ovaries similarly and were washed with H-TCM (15 mM Hepes-buffered tissue culture medium 199) supplemented with 100 IU/ml penicillin, 100 μg/ml streptomycin sulfate, and 0.03% (w/v) polyvinyl alcohol. The COCs were washed three times in H-TCM and were cultured in four-well multidishes in 500 μl of synthetic oviduct fluid medium [22] with 0.8% (w/v) bovine serum albumin (BSA fraction V), modified Eagle medium (MEM) nonessential amino acids (Gibco BRL, Burlington, ON, Canada), MEM essential amino acids (Gibco), 0.33 mM pyruvate, 50 μg/ml gentamicin, 1 mM glutamine, and 0.1 μg/ml recombinant human follicle-stimulating hormone (FSH; Gonaf F; Serono, Mississauga, ON, Canada).

### PDE Inhibitors

3-Isobutyl-methylxanthine (IBMX) is used as a broad-spectrum PDE inhibitor. It inhibits all PDE families, with the important exception of PDE8 and PDE9 (Table 1) [1]. Hence, IBMX-sensitive cAMP-PDE activity indicates the combined activities of PDE1, PDE2, PDE3, PDE4, PDE7, PDE10, and PDE11, whereas IBMX-insensitive cAMP-PDE activity reflects PDE8 activity [23–25]. IBMX-sensitive PDE5 and PDE6 and IBMX-insensitive PDE9 activities are absent from these groups because they specifically cleave cGMP [23] and then are not detected in the cAMP-PDE assay. Cilostamide (10 μM) and rolipram (10 μM) were used as specific PDE3 and PDE4 inhibitors, respectively, as described previously (Table 1) [26–28]. Dipyridamole was used as a moderately specific PDE8 inhibitor, with a reported half-maximal inhibitory concentration (IC<sub>50</sub>) of 4.5–9 μM for the PDE8 family (Table 1) [24, 29]. This is the best PDE8 inhibitor currently commercially available. Dipyridamole can also inhibit PDE7 (IC<sub>50</sub>, 9–42 μM) [30, 31], PDE10 (IC<sub>50</sub>, 1.2 μM) [32], and PDE11 (IC<sub>50</sub>, 0.82 μM) [30, 33] (Table 1). Dipyridamole was used at 10 μM (dose entirely inhibiting PDE10 and PDE11), 50 μM (dose additionally inhibiting PDE7 and PDE8), and 250 μM, where its significance is further addressed in *Discussion*.

### PDE Activity Measurement

The cAMP degradation assay was conducted according a method described previously [34]. Tissues were homogenized by freezing-thawing cycles in an hypotonic buffer (20 mM Tris-HCl, pH 7.4; 1 mM ethylene diaminetetraacetic acid; 0.2 mM ethylene glycol tetraacetic acid; 50 mM sodium fluoride; 50 mM benzamidine; 10 mM sodium pyrophosphate; 4 μg/ml aprotinin; 0.7 μg/ml pepstatin; 10 μg/ml soybean trypsin inhibitor; 0.5 μg/ml leupeptin, 2 mM PMSF; and 0.5% [v/v] Triton X-100). The homogenate was centrifuged for 20 min at 13000 × g to obtain the supernatant. The enzymatic activity was assessed using 1 μM cAMP as substrate, as described in previous studies [35]. Samples equivalent to 10 COCs or denuded oocytes per assay tube were used throughout the study. The sample volume was adjusted to 200 μl with Tris-BSA solution (40 mM Tris-HCl, pH 8.0; 10 mM MgCl<sub>2</sub>; 5 mM 2-mercaptoethanol; 0.75 mg/ml BSA fraction V; 1 μM cold cAMP; and 15 nM [<sup>3</sup>H]cAMP (1 × 10<sup>5</sup> cpm/tube and 30 Ci/mmol)) (GE Healthcare, Baie d'Urfe, QC, Canada). Reactions were incubated at 34°C for 15 min and boiled for 1 min. They were then treated with an excess of crotalus atrox venom (5'-nucleotidase; 50 μl, 1 mg/ml) and incubated for 20 min at 34°C. Adenosine was then separated from intact cAMP by anion-exchange chromatography followed by liquid scintillation quantification. Each measurement was done in triplicate within a single assay to account for intraassay variation. The experiment was performed independently at least three times.

TABLE 2. Primers used to perform PCR amplifications.

Gene	Primer	Primer sequences	Expected size of PCR product (bp)
<i>ACTB</i>	ACTB-F	5'-ATCCTGACCCTCAAGTACCCCAT-3'	242
	ACTB-R	5'-TACTCCTGCTTGTCTGATCCACAT-3'	
<i>PDE3A</i>	PDE3A-F	5'-TGTGGACATTCGCGTATGG-3'	235
	PDE3A-R	5'-TGGGAATAGCCAGCTTGTCTTTTTC-3'	
<i>PDE8A</i>	PDE8A-F	5'-AGCTGGCCATTCTCTACAACGACA-3'	295
	PDE8A-R	5'-TCTGGAGCCCTGAGCATGGTATTT-3'	
<i>PDE8B</i>	PDE8B-F	5'-TCCAATGCCTACCACAACCTCAC-3'	333
	PDE8B-R	5'-AATAATAGCCTGGCGCAGCGTTC-3'	
<i>PDE10A</i>	PDE10A-F	5'-GGACCACAGGGGCTTCAGTAAAC-3'	254
	PDE10A-R	5'-TGGTACATCTCTTCCAACCTGCTTCC-3'	
<i>PDE11A</i>	PDE11A-F	5'-CAAGTTTAAGGCAGCCAACATCCC-3'	234
	PDE11A-R	5'-GTTGAAGGCATGTCTCTCAGTTGTG-3'	

### RNA Extraction and RT-PCR

RNA extractions were performed with the RNeasy Mini Kit from Qiagen (Doncaster, Australia) according to the manufacturer's protocol. RNA samples were eluted in 15  $\mu$ l of elution buffer, followed by reverse transcription using the OmniScript RT Kit from Qiagen and poly(dT) from Ambion (Austin, TX). The primer pairs were designed according to bovine  $\beta$ -actin (*ACTB*; AY141970.1), porcine *PDE3A* (AY188088.1), bovine *PDE8A* (XM\_583282), human *PDE8B* (NM003719.1), human *PDE10A* (NM006661.1), and human *PDE11A* (NM016953.2) gene sequences in GenBank and were designed in evolutionarily conserved regions by comparison with available rodent sequences. Primer sequences and expected PCR product sizes are shown in Table 2. Primers were purchased from GeneWork (Adelaide, Australia). The PCR reactions were carried out in a 50- $\mu$ l reaction volume using HotStart Taq polymerase from Qiagen. Cycling conditions for all amplification reactions were as follows: 15 min at 95°C; 40 cycles of 1 min at 94°C, 1 min at 58°C, and 1 min at 72°C; and 10 min at 72°C. Positive controls were performed in parallel using mouse mammary gland (*ACTB*, *PDE8B*, *PDE10A*, and *PDE11A*) or bovine ovary cDNA (*PDE3A* and *PDE8A*) as the template. Additional amplifications were performed using *ACTB* primers on an equivalent amount of RNA to detect effects due to residual contamination with genomic DNA. Amplifications were visualized by 1% agarose gel electrophoresis and ethidium bromide staining. The PCR products were purified using a gel-purification kit (Qiagen), and they were sequenced to confirm their identity. *PDE3A*, *PDE8A*, *PDE8B*, *PDE10A*, and *PDE11A* PCR product sequences were, respectively, 100%, 100%, 99.4%, 99.5%, and 100% homologous to bovine predicted mRNA sequences (*PDE3A* [XM\_616776], *PDE8A* [XM\_583282], *PDE8B* [XM\_589274], *PDE10A* [XM\_582454], and *PDE11A* [XM\_001250426]).

### Western Blotting

Protein samples were prepared using the same hypotonic buffer described above. Protein samples were loaded on a 10% SDS-polyacrylamide gel for electrophoresis. Proteins were transferred to a Hybond-P membrane (GE Healthcare) using a Mini Protean 3 Cell apparatus (Bio-Rad Laboratories, Mississauga, ON, Canada). Membranes were blocked with TBS containing 0.1% (v/v) Tween-20 and 5% (w/v) nonfat dry milk. Membranes were blotted with the primary antibody *PDE8A* (diluted 1:500; FabGennix International Inc., Frisco, TX) at room temperature for 2 h, after which the membranes were exposed to goat anti-rabbit peroxidase-conjugated secondary antibody (diluted 1:40000; Jackson Immunoresearch Laboratories Inc., Bar Harbor, ME). *PDE8B* detection was performed using a *PDE8B* antibody (diluted 1:700; FabGennix International), followed by detection with a goat anti-rabbit peroxidase-conjugated secondary antibody (diluted 1:30000; Jackson Immunoresearch Laboratories). *PDE4D* detection was performed using a *PDE4D* antibody (diluted 1:200; Santa Cruz Biotechnologies, Santa Cruz, CA), followed by detection with a rabbit anti-goat peroxidase-conjugated secondary antibody (diluted 1:30000; Jackson Immunoresearch Laboratories). *PDE10A* detection was performed using a *PDE10A* antibody (diluted 1:700; Abcam, Cambridge, MA), followed by detection with a goat anti-rabbit peroxidase-conjugated secondary antibody (diluted 1:30000; Jackson Immunoresearch Laboratories). For  $\alpha$ -tubulin detection, a primary anti- $\alpha$ -tubulin antibody (Upstate, Charlottesville, VA) was diluted 1:50000 in TBS with 0.1% Tween-20. Membranes were blotted with a horseradish peroxidase-conjugated goat anti-mouse (diluted 1:20000; Upstate). Binding was detected using the ECL Plus kit (GE Healthcare) and exposed on autoradiographic films (GE Healthcare).

### cAMP Quantification

Quantification of cAMP was performed by radioimmunoassay using a validated method [36]. After 4 h of in vitro maturation (IVM), 10 COCs were collected, washed twice with H-TCM with 2 mM IBMX, put in 500  $\mu$ l of ethanol, and frozen in liquid nitrogen. Before cAMP quantification, samples were vortexed for 30 sec and centrifuged at 3000  $\times$  g for 20 min at 4°C. Supernatant was evaporated, resuspended in assay buffer (50 mM sodium acetate, pH 5.5), acetylated using triethanolamine and acetic anhydride (2:1), and assayed. [<sup>125</sup>I]-cAMP and cAMP antibody were added, and the reaction was incubated overnight at 4°C. The next morning, 1 ml of cold ethanol was added to the tubes, and they were centrifuged for 20 min at 3000  $\times$  g. The supernatants were discarded, and the pellets were counted in a gamma counter. Samples were done in duplicate and compared to a standard curve of known cAMP concentrations (0–1024 fmol cAMP).

### Oocyte Nuclear Maturation Assessment

Oocyte nuclear status was assessed by aceto-orcein staining as described previously [34]. Oocyte nuclear status was classified as 1) germinal vesicle (GV) stage if a GV could be observed; 2) MI stage if no GV could be seen and chromatin was either compacted or in a typical chessboard fashion; and 3) MII stage if the oocyte was displaying a chromatin configuration indicative of anaphase I, telophase I, or metaphase II.

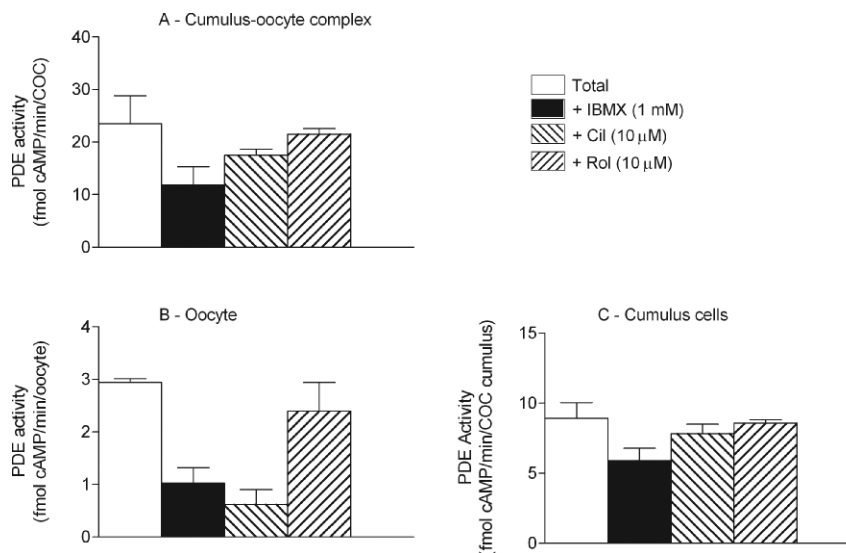
### In Vitro Fertilization and Embryo Culture

The COCs were recovered as described above. The basic medium for oocyte maturation was Bovine VitroMat (IVF Vet Solutions, Adelaide, Australia), a medium based on the ionic composition of bovine follicular fluid [37]. All IVM treatments were supplemented with 0.1 IU/ml FSH (Puregon; Organon, Oss, the Netherlands). Complexes were cultured in pre-equilibrated 300- $\mu$ l drops overlaid with mineral oil and incubated at 38.5°C with 6% CO<sub>2</sub> in humidified air for 24 or 30 h.

At specific IVM time intervals—namely, at either 24 or 30 h—COCs were removed from the control IVM wells or those containing dipyrindamole, washed twice using Bovine VitroWash (IVF Vet Solutions), and transferred to insemination dishes containing Bovine VitroFert (IVF Vet Solutions) supplemented with penicillamine (0.2 mM), hypotaurine (0.1 mM), and heparin (2 mg/ml). Frozen semen from a single bull of proven fertility (Semex, Guelph, ON, Canada) was used for inseminating all treated oocytes in all experiments. Briefly, thawed semen was layered over a discontinuous (45%:90%) Percoll gradient (Amersham Bioscience) and centrifuged at room temperature for 20–25 min at 700  $\times$  g. The supernatant was removed, and the sperm pellet was washed with 500  $\mu$ l of Bovine VitroWash and centrifuged for a further 5 min at 200  $\times$  g. Spermatozoa were resuspended with Bovine VitroFert, then added to the fertilization media drops (Bovine VitroFert supplemented with 0.01 mM heparin, 0.2 mM penicillamine, and 0.1 mM hypotaurine) at a final concentration of 1  $\times$  10<sup>6</sup> spermatozoa/ml. The COCs were inseminated at a density of 10  $\mu$ l of in vitro fertilization medium per COC for 24 h, at 39°C in 6% CO<sub>2</sub> in humidified air.

The cumulus cells were removed by gentle pipetting 23–24 h after insemination, and five presumptive zygotes were transferred into 20- $\mu$ l drops of pre-equilibrated Bovine VitroCleave (IVF Vet Solutions) and cultured under mineral oil at 38.5°C in 7% O<sub>2</sub>, 6% CO<sub>2</sub>, balance N<sub>2</sub>, for 5 days (Days 1–5). On Day 5, embryos were transferred in groups of five to six to 20- $\mu$ l drops of pre-equilibrated Bovine VitroBlast (IVF Vet Solutions) at 38.5°C and overlaid with mineral oil and were cultured to Day 8. Embryos were assessed for quality at

FIG. 1. The cAMP-PDE distribution in cumulus cells and oocytes. Cyclic AMP-PDE activity was measured in COCs (A), denuded oocytes (B), and cumulus cells (C). The results are presented as total cAMP-PDE activity and as cAMP-PDE activity inhibited by IBMX at 1 mM, inhibited by cilostamide at 10  $\mu$ M, and inhibited by rolipram at 10  $\mu$ M. The data presented are the mean  $\pm$  SEM of at least four replicates.



Day 8 according to the definitions presented in the Manual of the International Embryo Transfer Society [38] and were performed independently and in a blinded fashion by an experienced bovine embryologist.

### Statistical Analysis

Statistical analyses were conducted using Prism 5.00 GraphPad for Windows (GraphPad Software, San Diego, CA). Statistical significance was assessed by ANOVA, followed by either Dunnett (see Figures 6 and 7) or Bonferroni (see Figures 2, 3, and 8) multiple-comparison post hoc tests to identify individual differences between means. Probabilities of  $P < 0.05$  were considered statistically significant. All values are presented with their corresponding SEM.

## RESULTS

### cAMP-PDE in the Ovarian Follicle

The accepted distribution of PDE families in the mammalian ovarian follicle predicts *PDE3A* to be expressed in the oocyte and *PDE4D* in the mural granulosa cells [2, 5]. To validate this model in the bovine ovary, total cAMP-PDE activity was measured in COCs, cumulus cells, oocytes, and mural granulosa cells. This activity has been broken down into specific PDE family contributions by the use of family-specific inhibitors. The cAMP-PDE activity was inhibited with the broad-spectrum PDE inhibitor IBMX (1 mM), which inhibits all cAMP-PDE families except PDE8, as summarized in Table 1 [1]. By using cilostamide (PDE3 specific; 10  $\mu$ M) and rolipram (PDE4 specific; 10  $\mu$ M), the participation of these two important PDEs was measured in the ovarian follicle. The results of Figures 1–3 are summarized in Table 3. The cAMP-PDE activity measured in COCs was 25 fmol of cAMP hydrolyzed per minute per COC, from which only 50% was inhibited by IBMX, which targets cAMP-PDE families 1, 2, 3, 4, 7, 10, and 11 (Fig. 1A and Table 1). From this total activity, 26% was sensitive to cilostamide and 8% to rolipram, indicative of the presence of PDE3 and PDE4, respectively, in the COC (Fig. 1A). This level is surprisingly low, considering that PDE4 is thought to be the “granulosa/cumulus cell” PDE [5]. Moreover, 50% of the total cAMP-PDE activity remained in the presence of IBMX, consistent with the presence of PDE8.

Measurements performed on denuded bovine oocytes indicated that 80% of the total cAMP-PDE activity was inhibited by cilostamide, a PDE3 family-specific inhibitor, suggesting that the PDE3 family is the predominant type of

PDE in the oocyte (Fig. 1B). There was also a significant level of PDE activity in the presence of IBMX in the oocyte, supporting the expression of a PDE8 family member (Fig. 1B). Cumulus cell cAMP-PDE distribution revealed that only 35% of the activity was inhibited by IBMX, representing the contribution of PDE families 1, 2, 3, 4, 7, 10, and 11 (Fig. 1C). From the total PDE activity, less than 15% was inhibited by cilostamide and only 4% by rolipram, indicating the activities of PDE3 and PDE4, respectively. Consistent with the results obtained in the COCs, more than 60% of total PDE activity present in the cumulus cells was resistant to IBMX inhibition, strongly suggesting the expression of a PDE8 (Fig. 1C). These results support that PDE3 is the functionally predominant PDE in the oocyte, and PDE8 is the predominant family in cumulus cells.

To further understand cAMP modulation during oocyte meiotic resumption, PDE activities were measured in 1) COCs, 2) COC-cultured denuded oocytes, and 3) accompanying cumulus cells, after various time intervals around the time of oocyte meiotic resumption during IVM. Bovine COCs had significantly resumed meiosis after 8 h of IVM in our culture conditions ( $P < 0.001$ ; Fig. 2A). No significant changes in total PDE activity and PDE activity in the presence of IBMX (PDE8) were measured in COCs and cumulus cells in the first 9 h of IVM (Fig. 2, B and D). Measurements of PDE activities revealed that total PDE activity and PDE activity inhibited by cilostamide (PDE3) were not significantly different within the oocyte of cultured COCs during meiotic resumption (Fig. 2C). Other specific PDE family activities were measured in each sample and demonstrated that PDE activity in the presence of IBMX (PDE8) and PDE activities inhibited by cilostamide (PDE3) or inhibited by rolipram (PDE4) did not vary significantly during the first hours of IVM (Supplemental Fig. S1, available at [www.biolreprod.org](http://www.biolreprod.org)). These results suggest that cAMP-PDE activities are stable during meiotic resumption of the bovine COC.

Figure 3 shows the cAMP-PDE activity present in mural granulosa cells from follicles of 2–6 mm is 23 fmol of cAMP hydrolyzed per minute per microgram of protein. From this activity, more than 75% was inhibited by IBMX, whereas 25% was inhibited by cilostamide and 25% by rolipram. Interestingly, approximately 25% of the activity was measured in the presence of IBMX, indicating the presence of PDE8 (Fig. 3). By comparison, cAMP-PDE activity in mural granulosa cells from follicles larger than 10 mm was 63 fmol of cAMP

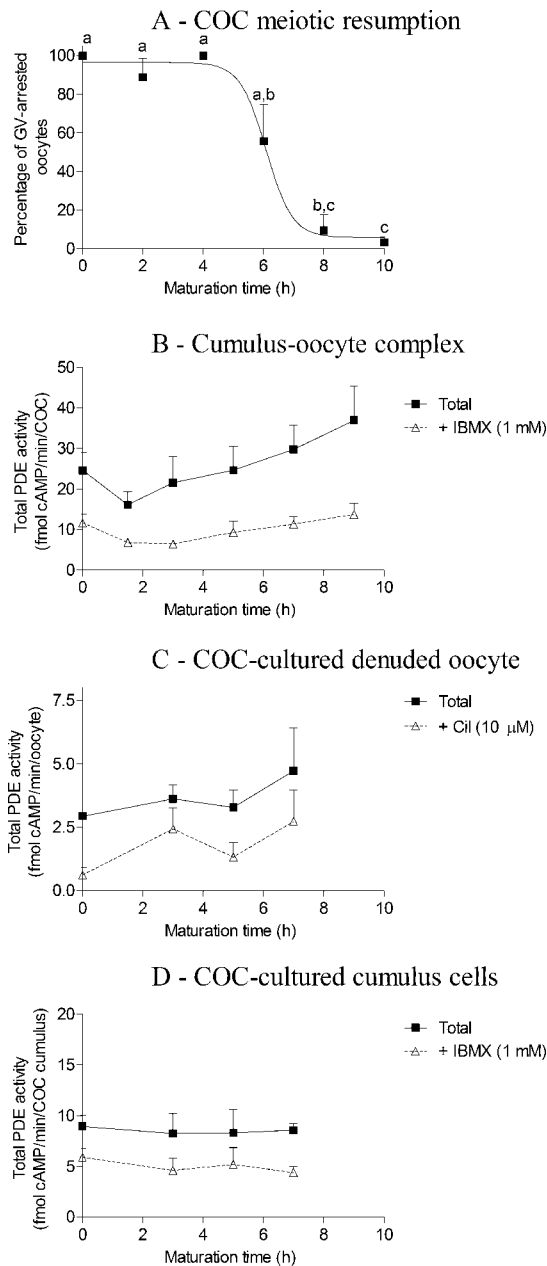


FIG. 2. The cAMP-PDE activity during IVM. A) Percentage of GV-arrested oocytes in FSH-stimulated IVM. Total cAMP-PDE activity was measured in COCs (B), COC-cultured denuded oocytes (C), and COC-cultured cumulus cells (D) at various time points during the initial hours of meiotic resumption. The data presented are the mean  $\pm$  SEM of at least three replicates. Different lowercase letters indicate a statistical difference between the means as determined by ANOVA followed by Bonferroni post hoc test. cil, cilostamide.

hydrolyzed per minute per microgram of protein, which is 2.7-fold higher than small-follicle granulosa cells ( $P < 0.001$ ). From this activity, less than 10% was inhibited by cilostamide (PDE3) and 20% by rolipram (PDE4). PDE activity measured in presence of IBMX was also increased significantly in large-follicle granulosa cells ( $P < 0.001$ ) and represented 45% of the total activity (Fig. 3). These results suggest that bovine mural granulosa cells have measurable PDE3, PDE4, and PDE8 activities, and that PDE8 is increased in granulosa cells from follicles larger than 10 mm compared with granulosa cells from 2- to 6-mm follicles (Table 3).

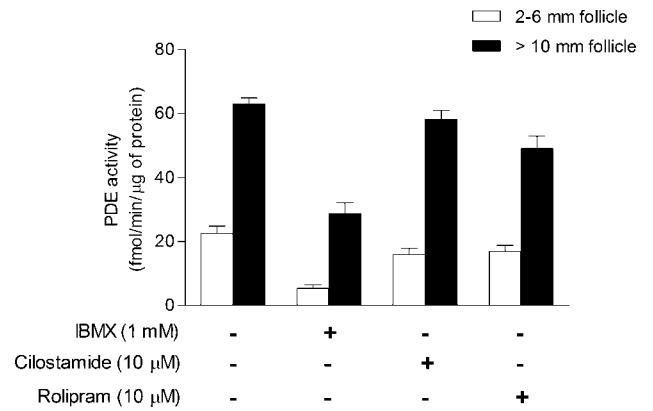


FIG. 3. The cAMP-PDE activity in mural granulosa cells of small and large follicles. Total cAMP-PDE activity was measured in homogenized mural granulosa cells from follicles of 2 to 6 mm (white bars) or from follicles of 10 mm and larger (black bars). The data represent the mean  $\pm$  SEM of at least three replicates.

To provide further evidence for the presence of various PDE activities in the ovarian follicle implicated above, the presence of transcripts of *PDE3A*, *PDE8A*, and *PDE8B*, as well as the recently discovered *PDE10A* and *PDE11A* [30, 39], were assessed by RT-PCR and immunoblotting in oocytes, cumulus cells, and mural granulosa cells. Figure 4 shows that the expression of *PDE3A* and *PDE8A* transcripts was detected in the oocyte (Fig. 4, top two blots). This result is consistent with the PDE3 and PDE8 activities measured in Figure 1B. The transcripts of *PDE8A*, *PDE8B*, and *PDE10A* were detected in cumulus cells (Fig. 4, second, third, and fourth blots), which correlates well with the large proportion of total PDE activity attributed to PDE8 (IBMX insensitive; Fig. 1C). Expression of *PDE8A* and *PDE8B* was also detected in mural granulosa cells (Fig. 4, second and third blots), in agreement with the IBMX-insensitive PDE activity measured in small-follicle granulosa cells (Fig. 3). *PDE11A* was not detected in any compartment of the ovarian follicle (Fig. 4). These results indicate that the bovine oocyte expresses *PDE3A* and *PDE8A*. Cumulus cells express *PDE8A*, *PDE8B*, and *PDE10A*, and mural granulosa cells express *PDE8A*.

Western blot experiments were conducted to characterize the expression profile of PDE proteins in the bovine ovarian follicle. Figure 5 shows that an immunoreactive band for PDE8A at the expected size of 100 kDa could be detected in mouse ovary and bovine testis positive controls, as well as in small-follicle granulosa cells and in COCs (Fig. 5A, top blot). PDE8B immunodetection also revealed immunoreactive bands at 89 kDa in rat brain, mouse ovary, bovine testis, granulosa cells from small follicles, and COCs (Fig. 5A, second blot). PDE10A was detected only in rat brain positive control at the expected size of about 95 kDa (Fig. 5A, third blot). Two immunoreactive PDE4D bands (75 kDa and 90 kDa) were detected in positive controls. However, only the 90-kDa immunoreactive band was detected in mural granulosa cells and COCs (Fig. 5A, fourth blot). Detection of  $\alpha$ -tubulin was performed as a loading control (Fig. 5A, fifth blot). Figure 5B shows that PDE8A: $\alpha$ -tubulin ratio is 65% higher in granulosa cells from large follicles compared with that from 2- to 6-mm follicles. These results show that PDE8A, PDE8B, and PDE4D were detected in granulosa cells from small follicles, and that PDE8A is increased in large follicles, which fully agrees with the PDE activity measurements in Figure 3 and RT-PCR experiments (Fig. 4). The COC was shown to express PDE4D, PDE8A, and PDE8B, which is in agreement with the PDE

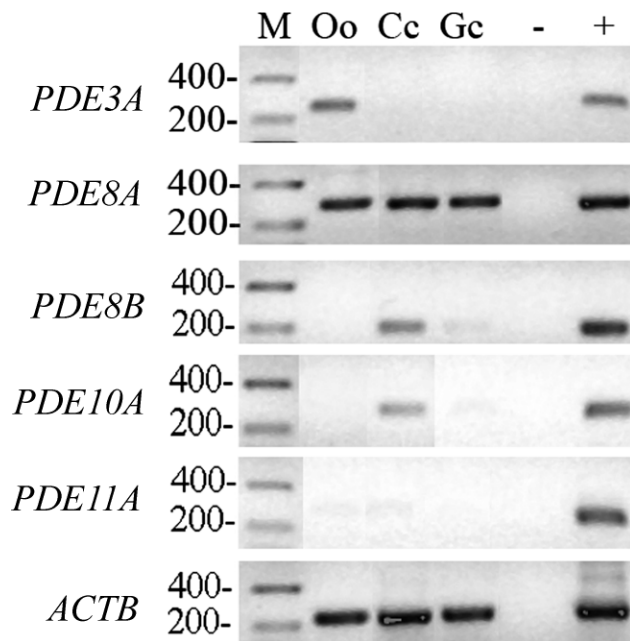


FIG. 4. Detection of *PDE3A*, *PDE8A*, *PDE8B*, *PDE10A*, *PDE11A*, and *ACTB* expression by RT-PCR in the various compartments of the ovarian follicle. For each gel, a molecular mass marker (M) was run with the samples, with the corresponding molecular weight (in base pairs) noted on the left. PDE genes were amplified from oocyte (Oo), cumulus (Cc), and granulosa cell (Gc) cDNA, along with a no-template negative control (-) and a mouse mammary gland positive control (+). A representative experiment of three replicates is shown.

activity measurements in Figure 1A. Overall, this set of results (Figs. 1–5) shows that 1) bovine oocytes have a high level of PDE3A and lower level of PDE8A; 2) cumulus cells have a high level of PDE8A and/or PDE8B and lower levels of PDE4D and PDE10A; and 3) that the functional activity of PDE in granulosa cells undergoes a developmental change during the course of follicular growth.

#### The Role of PDE8 on cAMP Degradation in the COC

As described above, cAMP-PDE activity measured in presence of IBMX refers to the PDE8 family (Table 1). The only known and commercially available inhibitor for the PDE8 family with an  $IC_{50}$  in the micromolar range is dipyridamole [24, 29]. To assess the potential role of PDE4 and PDE8 in the management of ovarian follicle cAMP, COCs were treated for 4 h with forskolin (100  $\mu$ M), an adenylyl cyclase stimulator, in combination with various doses of rolipram (10 and 100  $\mu$ M) or dipyridamole (10, 50, and 250  $\mu$ M). Figure 6 shows that forskolin treatment significantly increased cAMP in the COCs after 4 h of IVM. PDE4 inhibition using rolipram was unable to further increase its cAMP content, whereas inhibition using dipyridamole at a concentration of 50  $\mu$ M or higher led to a significant increase in cAMP in the COCs (Fig. 6). This further supports the notion that PDE8 is an important functional regulator of the intracellular content of cAMP in the COC and is more efficient than PDE4.

#### The Effect of PDE8 Inhibition on Oocyte Meiotic Maturation

It has been demonstrated that high levels of cAMP delay bovine oocyte meiotic maturation, and cumulus cells are major contributors to ooplasmic cAMP via intercellular gap-junc-

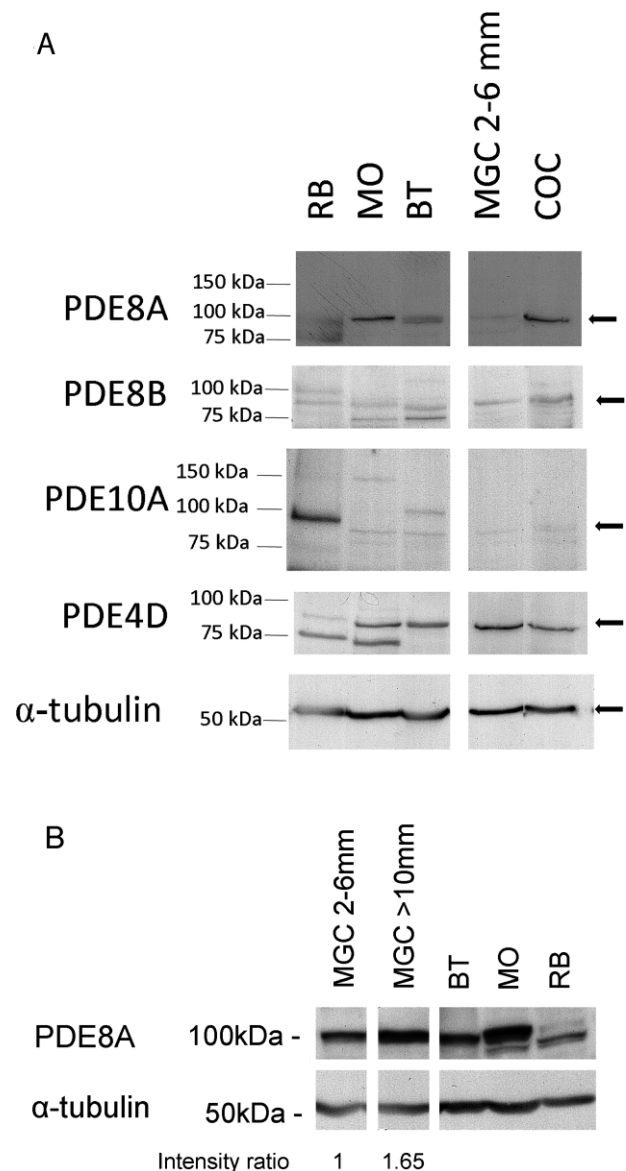


FIG. 5. Immunoblot detection of PDE8A, PDE8B, PDE10A, PDE4D, and  $\alpha$ -tubulin in granulosa cells and COCs. **A**) The expression of various PDEs was determined by immunodetection. Protein samples were run on SDS-PAGE and hybridized with specific PDE antibodies. For each gel, a molecular mass ladder was run with the samples, and band positions are displayed on the left in kiloDaltons. Samples are rat brain (RB), mouse ovary (MO), bovine testis (BT), mural granulosa cells (MGC) from 2- to 6-mm follicles, and COCs. **B**) Comparative expression of PDE8A between granulosa cells from 2- to 6-mm follicles and follicles larger than 10 mm. PDE8A and  $\alpha$ -tubulin intensities were quantified by ImageJ software (National Institutes of Health) from two separate experiments. The intensity ratio presented below the figure is expressed as the mean ratio between PDE8A and  $\alpha$ -tubulin.

tional communication [8, 40]. To verify the capacity of dipyridamole to delay cumulus-enclosed oocyte nuclear maturation, COCs were either cultured for 16 h alone, treated with forskolin, or treated with various PDE inhibitors. Figure 7A shows that 87% of control oocytes reached the metaphase II stage by 16 h. Increasing concentrations of dipyridamole did not significantly affect the proportion of oocytes reaching metaphase II (Fig. 7A). However, only 42% of forskolin-treated COCs progressed to the metaphase II stage (Fig. 7B). Interestingly, PDE4 inhibition in addition to forskolin had no further effect on meiotic maturation, whereas COCs treated

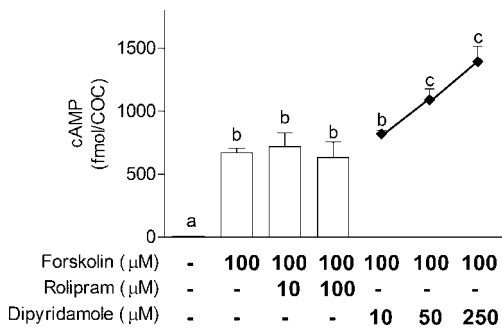


FIG. 6. The effect of an adenylyl cyclase stimulator in combination with PDE inhibitors on COC cAMP levels. The cAMP was measured in COCs after 4 h of IVM either after no stimulation or after forskolin (100 μM) treatment alone or in combination with rolipram (10 or 100 μM) or dipyridamole (10, 50, or 250 μM). The data represent the mean cAMP level per COC ± SEM of four replicates. Each measurement was conducted on 10 COCs. Different lowercase letters represent a statistical difference between the means as determined by ANOVA followed by Dunnett post hoc test.

with forskolin and a dipyridamole concentration of 50 μM or higher significantly impaired meiosis compared with forskolin-treated controls (10% vs. 42%;  $P < 0.05$ ). This experiment further demonstrates the physiological contribution of PDE8, in contrast to PDE4, on modulating a cAMP-regulated function of the COC.

The next experiment was designed to test whether dipyridamole could have an additive effect on IBMX-inhibited COC nuclear maturation. Because dipyridamole is targeting a PDE that IBMX cannot inhibit, its addition along with IBMX should delay GV breakdown even more than IBMX treatment alone. Our results in Figure 8 show that dipyridamole or IBMX treatment of COCs after 9 h of IVM led to a significant increase in GV-arrested oocytes and a decrease in oocytes at metaphase I (Fig. 8A). After 18 h, IBMX significantly increased metaphase I and decreased metaphase II percentages (Fig. 8B). No additive effect of dipyridamole on IBMX-treated COCs was observed at those two time points.

Thomas et al. [12] have demonstrated that PDE3 or PDE4 inhibition during oocyte maturation improved developmental potential of the oocyte, as shown by increased subsequent blastocyst yield. The present study has identified that PDE8 is also an important functional PDE in cumulus cells and in the oocyte. To elucidate a possible role for PDE8 in oocyte developmental competence, COCs were treated with or without 50 μM dipyridamole for 24 or 30 h of FSH-stimulated IVM, and they were subsequently subjected to in vitro fertilization and embryo development. First, the meiotic status of oocytes was assessed to evaluate the effect of dipyridamole on the kinetics of oocyte maturation. Figure 9 shows that COCs treated with dipyridamole had higher GV-arrested ( $P < 0.001$ ) and lower metaphase I percentages ( $P < 0.01$ ) after 9 h of IVM

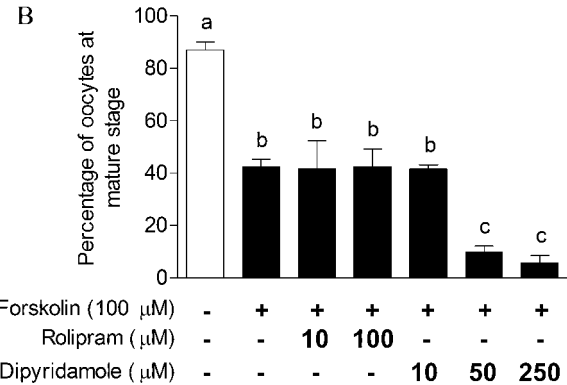
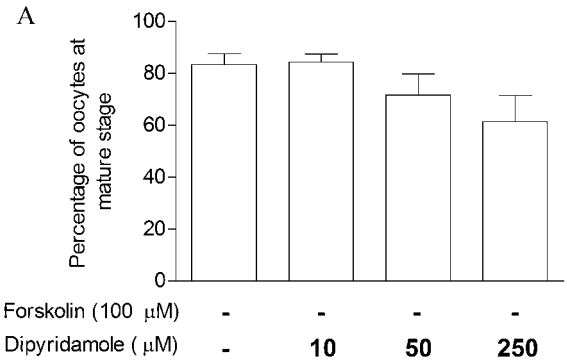


FIG. 7. The effect of an adenylyl cyclase stimulator and of PDE inhibitors on COC-cultured oocyte nuclear maturation. The effect of dipyridamole treatment alone (A) and of PDE inhibitors in the presence of forskolin (B) was investigated on COCs. After 16 h of IVM, COCs were denuded, fixed, and stained with aceto-orcein to assess the percentage of oocytes at the metaphase II (mature stage), as defined by a dense metaphase chromatin configuration and the extrusion of the first polar body. The data represent the mean metaphase II percentage ± SEM of three replicates. Each replicate had at least 25 COCs per treatment. Different lowercase letters represent a statistical difference between the means as determined by ANOVA followed by Dunnett post hoc test.

(Fig. 9, A and B). This effect of dipyridamole is carried on to later stages of oocyte maturation, as shown by dipyridamole's significant delaying effect on oocyte metaphase II percentage ( $P < 0.01$ ; Fig. 9C). After collection, COCs were cultured in control conditions or in presence of dipyridamole (50 μM). After IVM, they were subjected to in vitro fertilization and embryo development. The results in Figure 10A show that dipyridamole treatment significantly decreased the cleavage rate of oocytes fertilized after 30 h of IVM. Figure 10B shows a decreased blastocyst formation rate after dipyridamole treatment for 30 h of IVM compared with the untreated controls (24.3% vs. 56%;  $P < 0.01$ ). These results suggest that although PDE8 is the predominant PDE family in cumulus cells, its

TABLE 3. Relative distribution of cAMP-PDE activities in the bovine ovarian follicle.\*

Cell type	IBMX-sensitive PDEs			IBMX-insensitive PDE
	PDE3	PDE4	PDE1, PDE2, PDE7, PDE10, PDE11	PDE8
COC	25%	10%	15%	50%
Oocyte	80%	<5%	<5%	20%
Cumulus cells	15%	<5%	20%	60%
Mural GC—small follicle	25%	25%	25%	25%
Mural GC—large follicle	10%	20%	25%	45%

\* PDE5, PDE6, and PDE9 are not represented in this table since they degrade specifically cGMP.

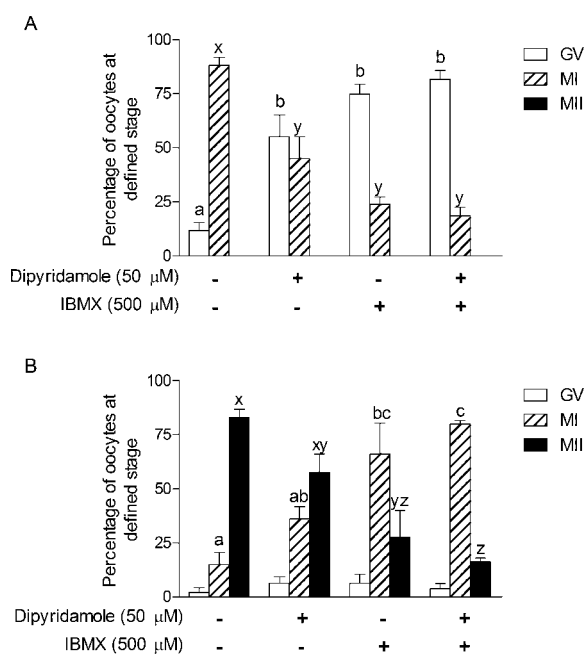


FIG. 8. The effect of dipyridamole and IBMX treatment on in vitro oocyte nuclear maturation. Bovine COCs were cultured with FSH for 9 h (A) and 18 h (B) either alone, with dipyridamole (50  $\mu$ M), with IBMX (500  $\mu$ M), or with a combination of the two. After culture, oocytes were denuded, stained with aceto-orcein, and classified as GV-arrested (GV), metaphase I (MI), or metaphase II (MII). The data represent the mean percentage of oocytes at a certain stage  $\pm$  SEM of four replicates. Each replicate had at least 20 COCs per treatment. Different letters above the bars represent a statistical difference between the means as determined by ANOVA followed by Bonferroni post hoc test.

continuous inhibition by dipyridamole during the course of oocyte maturation does not promote oocyte cytoplasmic maturation and developmental competence.

## DISCUSSION

The present study has investigated the distribution and role of the various PDE families present in the bovine ovarian follicle. Our results have shown that 1) *PDE3A* is the predominant PDE family expressed and functional in the oocyte; 2) two PDEs not inhibited by IBMX—*PDE8A* and *PDE8B*—are the predominant PDEs expressed in the cumulus cells, along with low levels of *PDE4D*; and 3) that mural granulosa cells express mainly *PDE4D*, *PDE8A*, and *PDE8B*, with changes in relative activities during follicular growth (Table 3). Inhibiting the activities of the novel ovarian PDEs—*PDE8* and *PDE10*—in cumulus cells by using dipyridamole increased cAMP levels in the COCs and delayed oocyte nuclear maturation. Together, these results give a new perspective on the accepted distribution of PDE families in the ovarian follicle and open the door to new avenues of hormonal and pharmacological manipulation of follicle growth and ovulation [41].

The current study provides the first demonstration of a functional role for *PDE8A* and *PDE8B* in the mammalian ovary. Measurements of cumulus cell PDE activity revealed that surprisingly little (<5%) was inhibited by rolipram (*PDE4*), and 60% was not inhibited by IBMX (Table 3). *PDE8* is the only cAMP-PDE that cannot be inhibited by IBMX (Table 1). Therefore, any PDE activity measured in the presence of IBMX can only be attributed to *PDE8A* and/or *PDE8B* activity [24, 29]. This PDE activity, resistant to IBMX

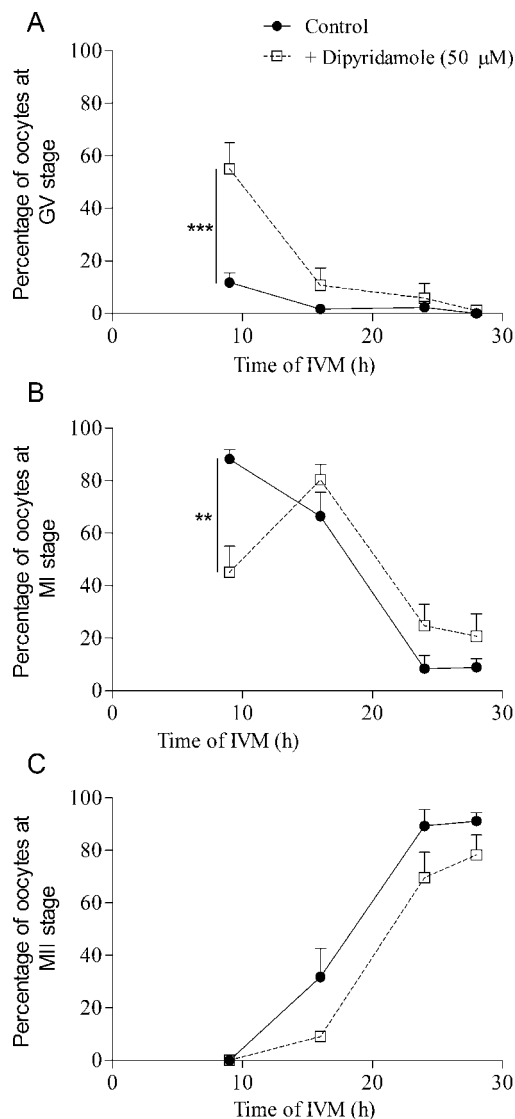


FIG. 9. The effect of dipyridamole treatment of COCs on oocyte nuclear maturation. Bovine COCs were cultured with FSH for 9, 16, 24, or 28 h either alone or together with dipyridamole (50  $\mu$ M). After culture, oocyte nuclear status was assessed and classified as GV-arrested (A), metaphase I (B), or metaphase II (C). The data represent the mean  $\pm$  SEM of four replicates. Statistical analysis was performed by ANOVA followed by Bonferroni post hoc test. \*\* $P < 0.01$ , \*\*\* $P < 0.001$ .

inhibition in cumulus and granulosa cells, is the first evidence of the presence of *PDE8* activity in the ovary, and it challenges the notion that *PDE4* is the major granulosa cell PDE [5, 42]. This conclusion is further supported by the detection of *PDE8A* and *PDE8B* by RT-PCR and Western blotting. A previous study showed that subcutaneous injection of *PDE4* inhibitors alone or in combination with low doses of human chorionic gonadotropin could induce ovulation in rats [41]. This study provided an interesting approach to decrease the hormonal doses required for superovulation protocols. However, *PDE4* inhibitors are of very limited selectivity over the four genes of the family, and *PDE4* is widely expressed throughout the body, which raises the likelihood of treatment side effects [23]. The present study is reporting *PDE8* activity in ovarian follicular somatic cells and offers a novel target for pharmaceutical modulation of gonadotropin stimulation. Although its expression was highest in testis and liver, *PDE8A*



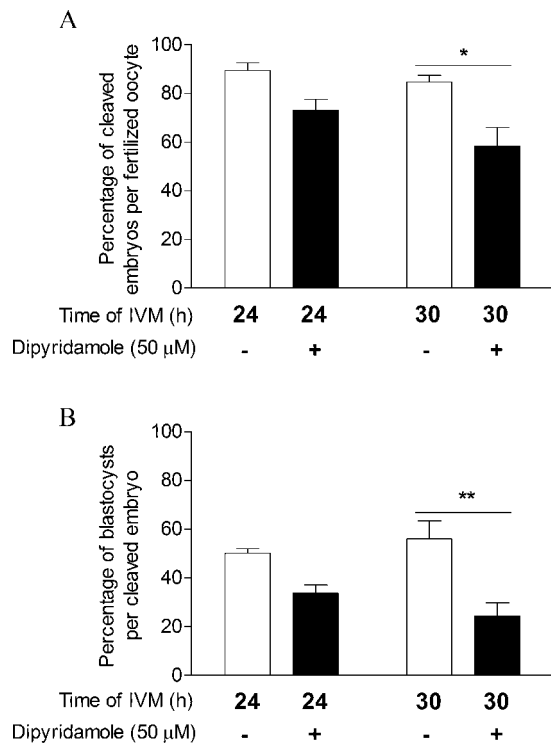


FIG. 10. The effect of dipyrindamole treatment of COCs during IVM on oocyte developmental capacity. Bovine COCs were cultured with FSH for 24 or 30 h alone or together with dipyrindamole (50 μM). Oocytes were then submitted to in vitro fertilization and embryo development. Oocyte developmental capacity was assessed by the cleavage rate (A) and the blastocyst rate on Day 8 (B). The data represent the mean  $\pm$  SEM of three replicates. Statistical analysis was performed by ANOVA followed by Bonferroni post hoc test. \* $P < 0.05$ , \*\* $P < 0.01$ .

was shown to be expressed in human [29] and mouse ovary by Northern blotting [24]. The highest level of *PDE8B* was observed in the thyroid gland and also in rat ovary [43] and, at low levels, in human ovary [44]. This restricted expression pattern could potentially allow PDE8 inhibition to be used to increase gonadotropin sensitivity of the ovary while limiting side effects to other organs.

Among all of the PDE inhibitors available, only dipyrindamole has been shown to inhibit PDE8, with an  $IC_{50}$  ranging from 4 to 9 μM [24, 29]. Previous studies have used dipyrindamole at 100 μM to suggest the presence of PDE8 in kidney and leukocytes [45, 46]. Here, dipyrindamole at 50 μM increased COC cAMP and delayed oocyte maturation (Figs. 3 and 4), and this can likely be attributed to inhibition of cumulus cell PDE8 and PDE10. From the group of four PDEs inhibited by dipyrindamole (PDEs 7, 8, 10, and 11; Table 3), only PDE8 and PDE10 are present in cumulus cells (present study), whereas only a weak signal for PDE7 was detected in mouse ovary [31], and PDE11 was not detected (present study). Furthermore, PDE7 and PDE10 are likely to contribute a minor role, because the combined activities of PDE1, PDE2, PDE7, PDE10, and PDE11 represented only 20% of total cumulus cell PDE activity (Table 3). Hence, the effect of dipyrindamole on COC functions is likely to be principally due to inhibition specifically of PDE8. The explanation for the lack of additive effect of the combination of IBMX and dipyrindamole on oocyte nuclear maturation (Fig. 8) remains to be determined. However, these data provide various lines of evidence that PDE8 is a critical PDE for cAMP management in the ovarian follicle.

The PDE3 activity present in the oocyte reported in the present study is supported by previously published literature showing that PDE3 inhibition increased cAMP in the bovine oocyte and delayed oocyte meiotic resumption and progression [8, 47, 48]. It also is similar to findings in the rat and pig, where PDE3 activity was measured and found to be the predominant cAMP-degradation enzyme in the oocyte [34, 49]. Interestingly, although the total cAMP-PDE activity in COCs is different, the total cAMP-PDE activity in the oocyte is similar for the three species ( $\sim 3$  fmol/min per oocyte) [34, 49]. The presence in the oocyte of an IBMX-resistant PDE8 activity, as reported here, has not been investigated previously in any other species. Two studies have shown that intraperitoneal or subcutaneous injection of PDE3 inhibitors in mice and oral administration of a PDE3 inhibitor in *Rhesus macaque* prevented in vivo oocyte maturation [50, 51]. The present results show that PDE8 inhibition prevents oocyte maturation in vitro. PDE8-specific inhibition could be considered as an alternative to PDE3 for contraception, because PDE3 inhibitors have significant negative side effects, including tachycardia, which has held back its clinical applicability [50].

PDE8s and PDE3s have similar affinities for cAMP ( $K_m$ , 0.04–0.06 μM vs. 0.02–0.15 μM, respectively) [23], suggesting that PDE8 expression in bovine oocytes would not change cAMP-degradation kinetics compared with other species where PDE3 alone is in the oocyte. However, PDE8s have approximately a 100-fold higher affinity for cAMP than PDE4s ( $K_m$ , 0.04–0.06 μM vs. 1.2–5.9 μM, respectively) [23], meaning that the presence of PDE8 in bovine cumulus cells could lead to a different cAMP basal level and cAMP management upon stimulation and could contribute to the rapid spontaneous meiotic resumption discussed above. It has to be kept in mind that the relatively high  $K_m$  of PDE4 for cAMP may lead to a certain underestimation of PDE4 levels, because these experiments were conducted using 1 μM cAMP as a substrate in the PDE assay, a concentration at which PDE4 activity might not be maximal. However, this method has been used widely for PDE activity assessment, often to study PDE4 specifically [52–54]. It is worth noting that the level of cAMP-PDE activity measured in the bovine COC before IVM (25 fmol cAMP  $min^{-1}$   $COC^{-1}$ ) is about 2-fold higher than in a porcine COC (12 fmol cAMP  $min^{-1}$   $COC^{-1}$ ) [26]. Interestingly, porcine cumulus cells upregulate *PDE3A*, a low- $K_m$  cAMP-PDE, in response to gonadotropin stimulation [26]. The physiological significance of this fact remains to be elucidated, but it appears that cumulus cells tend to acquire PDE subtypes that allow them to maintain a low basal cAMP level.

The present results have shown that dipyrindamole treatment increases cAMP and delays oocyte maturation, but it does not improve oocyte developmental capacity. Thomas et al. [12] have shown that PDE3-specific or PDE4-specific inhibition of FSH-treated bovine COCs significantly increased blastocyst development rate and cell number compared with FSH-treated COCs [12]. These results suggest that subtle PDE4 inhibition (<5% of total PDE activity in the cumulus), rather than broad inhibition using IBMX or more specific inhibition using dipyrindamole, is a better way to improve oocyte quality. It is important to keep in mind that dipyrindamole is not only acting on PDE8 but also on PDE10, both of which are present in cumulus cells. Although this result contradicts our initial hypothesis, it might be indicative of a more profound physiologic significance of PDE4 and PDE8. Inhibition of PDE8 might negatively affect essential cumulus cell functions, such as gap-junction communication, cell signaling, or supply of metabolites for oocyte or cumulus expansion. To dissect

these possibilities, the development of specific PDE8 inhibitors would be required.

In conclusion, this study is the first to characterize the presence of and describe a functional role for PDE8 in the mammalian ovary. Cumulus cells were shown to express significant amounts of PDE8A and PDE8B, as demonstrated by PDE assay, RT-PCR, and Western blot experiments. Granulosa cells from small follicles were shown to express *PDE8A*, *PDE8B*, and *PDE4D*, and to significantly alter the relative contribution of these PDEs during follicle growth. This suggests that granulosa cells display a distinct developmentally regulated PDE activity pattern during follicular growth. The oocyte was shown to express predominantly *PDE3A* but also *PDE8A*. PDE8 inhibition using dipyrindamole increased COC cAMP and delayed oocyte nuclear maturation, although oocyte developmental capacity was not improved. This study highlights the need to carefully investigate the PDE expression pattern of follicular cell types in other species, especially primates. This is particularly relevant, given the ongoing interest in using specific PDE inhibitors as novel forms of nonsteroidal contraceptives [50, 51], and that such an approach is based largely on a rodent ovarian model of PDE cell-specific expression.

## ACKNOWLEDGMENTS

The authors would like to thank Isabelle Laflamme for her professional technical assistance. The authors are also grateful to Professor David T. Armstrong and Fred Amato for assistance with cAMP radioimmunoassay, and A/Professor Jeremy G. Thompson for embryology expertise.

## REFERENCES

- Conti M, Beavo J. Biochemistry and physiology of cyclic nucleotide phosphodiesterases: essential components in cyclic nucleotide signaling. *Annu Rev Biochem* 2007; 76:481–511.
- Tsafiri A, Chun SY, Zhang R, Hsueh AJ, Conti M. Oocyte maturation involves compartmentalization and opposing changes of cAMP levels in follicular somatic and germ cells: studies using selective phosphodiesterase inhibitors. *Dev Biol* 1996; 178:393–402.
- Jin SL, Richard FJ, Kuo WP, D'Ercole AJ, Conti M. Impaired growth and fertility of cAMP-specific phosphodiesterase PDE4D-deficient mice. *Proc Natl Acad Sci U S A* 1999; 96:11998–12003.
- Masciarelli S, Horner K, Liu C, Park SH, Hinckley M, Hockman S, Nedachi T, Jin C, Conti M, Manganiello V. Cyclic nucleotide phosphodiesterase 3A-deficient mice as a model of female infertility. *J Clin Invest* 2004; 114:196–205.
- Conti M, Andersen CB, Richard F, Mehats C, Chun SY, Horner K, Jin C, Tsafiri A. Role of cyclic nucleotide signaling in oocyte maturation. *Mol Cell Endocrinol* 2002; 187:153–159.
- Jessus C, Ozon R. How does *Xenopus* oocyte acquire its competence to undergo meiotic maturation? *Biol Cell* 2004; 96:187–192.
- Pincus G, Enzmann EV. The comparative behaviour of mammalian eggs in vivo and in vitro. *J Exp Med* 1935; 62:665–675.
- Thomas RE, Armstrong DT, Gilchrist RB. Differential effects of specific phosphodiesterase isoenzyme inhibitors on bovine oocyte meiotic maturation. *Dev Biol* 2002; 244:215–225.
- Greve T, Xu KP, Callesen H, Hyttel P. In vivo development of in vitro fertilized bovine oocytes matured in vivo versus in vitro. *J In Vitro Fert Embryo Transf* 1987; 4:281–285.
- Leibfried-Rutledge ML, Critser ES, Eyestone WH, Northey DL, First NL. Development potential of bovine oocytes matured in vitro or in vivo. *Biol Reprod* 1987; 36:376–383.
- Lonergan P, Rizos D, Gutierrez-Adan A, Fair T, Boland MP. Oocyte and embryo quality: effect of origin, culture conditions and gene expression patterns. *Reprod Domest Anim* 2003; 38:259–267.
- Thomas RE, Thompson JG, Armstrong DT, Gilchrist RB. Effect of specific phosphodiesterase isoenzyme inhibitors during in vitro maturation of bovine oocytes on meiotic and developmental capacity. *Biol Reprod* 2004; 71:1142–1149.
- Thomas RE, Armstrong DT, Gilchrist RB. Bovine cumulus cell-oocyte gap junctional communication during in vitro maturation in response to manipulation of cell-specific cyclic adenosine 3',5'-monophosphate levels. *Biol Reprod* 2004; 70:548–556.
- Laforest MF, Pouliot E, Gueguen L, Richard FJ. Fundamental significance of specific phosphodiesterases in the control of spontaneous meiotic resumption in porcine oocytes. *Mol Reprod Dev* 2005; 70:361–372.
- Nogueira D, Cortvrindt R, De Matos DG, Vanhouste L, Smitz J. Effect of phosphodiesterase type 3 inhibitor on developmental competence of immature mouse oocytes in vitro. *Biol Reprod* 2003; 69:2045–2052.
- Aktas H, Wheeler MB, Rosenkrans CF Jr, First NL, Leibfried-Rutledge ML. Maintenance of bovine oocytes in prophase of meiosis I by high [cAMP]<sub>i</sub>. *J Reprod Fertil* 1995; 105:227–235.
- Barretto LS, Caiado Castro VS, Garcia JM, Mingoti GZ. Role of roscovitine and IBMX on kinetics of nuclear and cytoplasmic maturation of bovine oocytes in vitro. *Anim Reprod Sci* 2007; 99:202–207.
- Sirard MA, First NL. In vitro inhibition of oocyte nuclear maturation in the bovine. *Biol Reprod* 1988; 39:229–234.
- Shu YM, Zeng HT, Ren Z, Zhuang GL, Liang XY, Shen HW, Yao SZ, Ke PQ, Wang NN. Effects of cilostamide and forskolin on the meiotic resumption and embryonic development of immature human oocytes. *Hum Reprod* 2008; 23:504–513.
- Lonergan P, Khatir H, Carolan C, Mermillod P. Bovine blastocyst production in vitro after inhibition of oocyte meiotic resumption for 24 h. *J Reprod Fertil* 1997; 109:355–365.
- Saeki K, Nagao Y, Kishi M, Nagai M. Developmental capacity of bovine oocytes following inhibition of meiotic resumption by cycloheximide or 6-dimethylaminopurine. *Theriogenology* 1997; 48:1161–1172.
- Ali A, Sirard MA. Effect of the absence or presence of various protein supplements on further development of bovine oocytes during in vitro maturation. *Biol Reprod* 2002; 66:901–905.
- Bender AT, Beavo JA. Cyclic nucleotide phosphodiesterases: molecular regulation to clinical use. *Pharmacol Rev* 2006; 58:488–520.
- Soderling SH, Bayuga SJ, Beavo JA. Cloning and characterization of a cAMP-specific cyclic nucleotide phosphodiesterase. *Proc Natl Acad Sci U S A* 1998; 95:8991–8996.
- Soderling SH, Bayuga SJ, Beavo JA. Identification and characterization of a novel family of cyclic nucleotide phosphodiesterases. *J Biol Chem* 1998; 273:15553–15558.
- Sasseville M, Cote N, Vigneault C, Guillemette C, Richard FJ. 3',5'-cyclic adenosine monophosphate-dependent up-regulation of phosphodiesterase type 3A in porcine cumulus cells. *Endocrinology* 2007; 148:1858–1867.
- Hidaka H, Hayashi H, Kohri H, Kimura Y, Hosokawa T, Igawa T, Saitoh Y. Selective inhibitor of platelet cyclic adenosine monophosphate phosphodiesterase, cilostamide, inhibits platelet aggregation. *J Pharmacol Exp Ther* 1979; 211:26–30.
- Schwabe U, Miyake M, Ohga Y, Daly JW. 4-(3-Cyclopentyl-4-methoxyphenyl)-2-pyrrolidone (ZK 62711): a potent inhibitor of adenosine cyclic 3',5'-monophosphate phosphodiesterases in homogenates and tissue slices from rat brain. *Mol Pharmacol* 1976; 12:900–910.
- Fisher DA, Smith JF, Pillar JS, St Denis SH, Cheng JB. Isolation and characterization of PDE8A, a novel human cAMP-specific phosphodiesterase. *Biochem Biophys Res Commun* 1998; 246:570–577.
- Hetman JM, Robas N, Baxendale R, Fidock M, Phillips SC, Soderling SH, Beavo JA. Cloning and characterization of two splice variants of human phosphodiesterase 11A. *Proc Natl Acad Sci U S A* 2000; 97:12891–12895.
- Hetman JM, Soderling SH, Glavas NA, Beavo JA. Cloning and characterization of PDE7B, a cAMP-specific phosphodiesterase. *Proc Natl Acad Sci U S A* 2000; 97:472–476.
- Soderling SH, Bayuga SJ, Beavo JA. Isolation and characterization of a dual-substrate phosphodiesterase gene family: PDE10A. *Proc Natl Acad Sci U S A* 1999; 96:7071–7076.
- Fawcett L, Baxendale R, Stacey P, McGrouther C, Harrow I, Soderling S, Hetman J, Beavo JA, Phillips SC. Molecular cloning and characterization of a distinct human phosphodiesterase gene family: PDE11A. *Proc Natl Acad Sci U S A* 2000; 97:3702–3707.
- Sasseville M, Cote N, Guillemette C, Richard FJ. New insight into the role of phosphodiesterase 3A in porcine oocyte maturation. *BMC Dev Biol* 2006; 6:47.
- Thompson WJ, Terasaki WL, Epstein PM, Strada SJ. Assay of cyclic nucleotide phosphodiesterase and resolution of multiple molecular forms of the enzyme. *Adv Cyclic Nucleotide Res* 1979; 10:69–92.
- Reddoh RB, Pelletier RM, Barbe GJ, Armstrong DT. Lack of ovarian responsiveness to gonadotropic hormones in infantile rats sterilized with busulfan. *Endocrinology* 1986; 119:879–886.
- Sutton-McDowall ML, Gilchrist RB, Thompson JG. Effect of hexoses and gonadotrophin supplementation on bovine oocyte nuclear maturation

- during in vitro maturation in a synthetic follicle fluid medium. *Reprod Fertil Dev* 2005; 17:407–415.
38. Stingfellow DA, Seidel SM. *Manual of the International Embryo Transfer Society*. Savoy, IL: International Embryo Transfer Society; 1998.
  39. Fujishige K, Kotera J, Michibata H, Yuasa K, Takebayashi S, Okumura K, Omori K. Cloning and characterization of a novel human phosphodiesterase that hydrolyzes both cAMP and cGMP (PDE10A). *J Biol Chem* 1999; 274:18438–18445.
  40. Luciano AM, Modina S, Vassena R, Milanese E, Lauria A, Gandolfi F. Role of intracellular cyclic adenosine 3',5'-monophosphate concentration and oocyte-cumulus cells communications on the acquisition of the developmental competence during in vitro maturation of bovine oocyte. *Biol Reprod* 2004; 70:465–472.
  41. McKenna SD, Pietropaolo M, Tos EG, Clark A, Fischer D, Kagan D, Bao B, Chedrese PJ, Palmer S. Pharmacological inhibition of phosphodiesterase 4 triggers ovulation in follicle-stimulating hormone-primed rats. *Endocrinology* 2005; 146:208–214.
  42. Conti M. Specificity of the cyclic adenosine 3',5'-monophosphate signal in granulosa cell function. *Biol Reprod* 2002; 67:1653–1661.
  43. Kobayashi T, Gamanuma M, Sasaki T, Yamashita Y, Yuasa K, Kotera J, Omori K. Molecular comparison of rat cyclic nucleotide phosphodiesterase 8 family: unique expression of PDE8B in rat brain. *Gene* 2003; 319:21–31.
  44. Hayashi M, Matsushima K, Ohashi H, Tsunoda H, Murase S, Kawarada Y, Tanaka T. Molecular cloning and characterization of human PDE8B, a novel thyroid-specific isozyme of 3',5'-cyclic nucleotide phosphodiesterase. *Biochem Biophys Res Commun* 1998; 250:751–756.
  45. Jackson EK, Ren J, Zacharia LC, Mi Z. Characterization of renal ecto-phosphodiesterase. *J Pharmacol Exp Ther* 2007; 321:810–815.
  46. Dong H, Osmanova V, Epstein PM, Brocke S. Phosphodiesterase 8 (PDE8) regulates chemotaxis of activated lymphocytes. *Biochem Biophys Res Commun* 2006; 345:713–719.
  47. Bilodeau-Goeseels S. Effects of phosphodiesterase inhibitors on spontaneous nuclear maturation and cAMP concentrations in bovine oocytes. *Theriogenology* 2003; 60:1679–1690.
  48. Mayes MA, Sirard MA. Effect of type 3 and type 4 phosphodiesterase inhibitors on the maintenance of bovine oocytes in meiotic arrest. *Biol Reprod* 2002; 66:180–184.
  49. Richard FJ, Tsafirri A, Conti M. Role of phosphodiesterase type 3A in rat oocyte maturation. *Biol Reprod* 2001; 65:1444–1451.
  50. Wiersma A, Hirsch B, Tsafirri A, Hanssen RG, Van de Kant M, Kloosterboer HJ, Conti M, Hsueh AJ. Phosphodiesterase 3 inhibitors suppress oocyte maturation and consequent pregnancy without affecting ovulation and cyclicity in rodents. *J Clin Invest* 1998; 102:532–537.
  51. Jensen JT, Zelinski MB, Stanley JE, Fanton JW, Stouffer RL. The phosphodiesterase 3 inhibitor ORG 9935 inhibits oocyte maturation in the naturally selected dominant follicle in rhesus macaques. *Contraception* 2008; 77:303–307.
  52. Bartsch O, Bartlick B, Ivell R. Phosphodiesterase 4 inhibition synergizes with relaxin signaling to promote decidualization of human endometrial stromal cells. *J Clin Endocrinol Metab* 2004; 89:324–334.
  53. Campos-Toimil M, Keravis T, Orallo F, Takeda K, Lugnier C. Short-term or long-term treatments with a phosphodiesterase-4 (PDE4) inhibitor result in opposing agonist-induced Ca(2+) responses in endothelial cells. *Br J Pharmacol* 2008; 154:82–92.
  54. Lynch MJ, Baillie GS, Mohamed A, Li X, Maisonneuve C, Klusmann E, van Heeke G, Houslay MD. RNA silencing identifies PDE4D5 as the functionally relevant cAMP phosphodiesterase interacting with beta arrestin to control the protein kinase A/AKAP79-mediated switching of the beta2-adrenergic receptor to activation of ERK in HEK293B2 cells. *J Biol Chem* 2005; 280:33178–33189.